

Statistica Sinica Preprint No: SS-2023-0246

Title	Simultaneous Inference for the Distribution of Functional Principal Component Scores
Manuscript ID	SS-2023-0246
URL	http://www.stat.sinica.edu.tw/statistica/
DOI	10.5705/ss.202023.0246
Complete List of Authors	Leheng Cai and Qirui Hu
Corresponding Authors	Qirui Hu
E-mails	hqr20@mails.tsinghua.edu.cn
Notice: Accepted version subject to English editing.	

SIMULTANEOUS INFERENCE FOR THE DISTRIBUTION OF FUNCTIONAL PRINCIPAL COMPONENT SCORES

Leheng Cai¹, Qirui Hu¹

Tsinghua University

Abstract: This paper introduces a novel methodology for simultaneous inference of the cumulative distribution function (CDF) of functional principal component (FPC) scores. We establish a general framework for estimating the CDF, including both nonsmooth and smooth estimators, and demonstrate their asymptotic equivalence. For dense functional data, we employ nonparametric pre-smoothing, ensuring oracle properties that make our estimators equivalent to those from fully observed trajectories. We recommend B-spline smoothing for its computational efficiency. Additionally, we derive theoretical properties to construct simultaneous confidence bands (SCBs) and develop new testing procedures for the distribution of FPC scores. These procedures, including Kolmogorov-Smirnov and Cramér-von Mises tests, can handle a diverging number of components and are particularly effective for testing the normality of functional data, a common assumption in literature and practice. Our methodology is supported by extensive numerical simulations and applied to well-known functional datasets and Electroencephalogram (EEG) data.

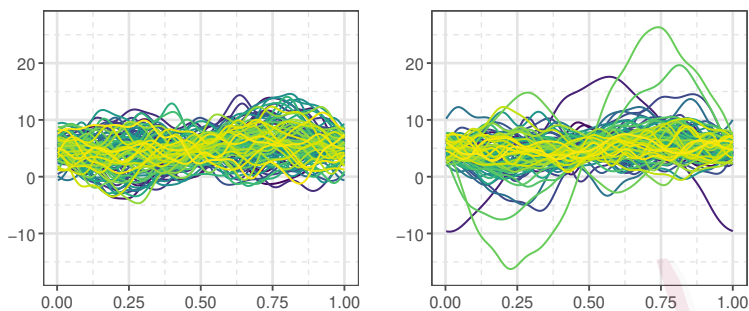
Key words and phrases: Cumulative distribution function, Functional principal component scores, Goodness of fit tests, Nonparametric smoothing, Simultaneous inference.

1. Introduction

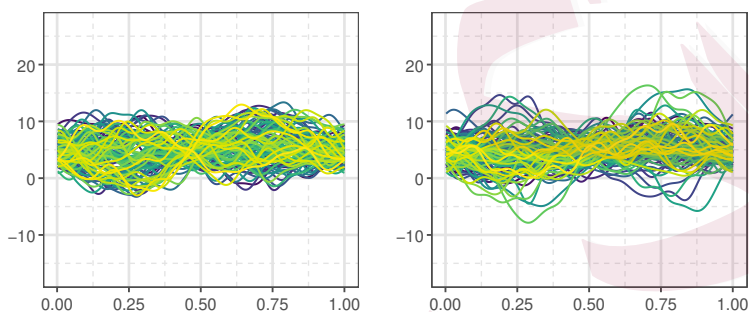
Functional data analysis, a key area in statistics applied in finance, environment, and neuroscience; see Bosq (2000), Hsing and Eubank (2015), deals with variables as random functions over a domain. Despite the infinite dimensionality of these functions offering rich information, it poses challenges in pattern identification and signal extraction. Functional principal component analysis (FPCA), as detailed in Yao et al. (2005b), Berkes et al. (2009), and Zhang et al. (2011), is crucial in dimension reduction and is widely used in functional data analysis, including functional linear models and change point analysis.

While there is extensive research on the eigenvalues and eigenfunctions of functional data; see Dauxois et al. (1982), Hall and Hosseini-Nasab (2009), Kokoszka and Reimherr (2013), Cai and Hu (2024), statistical inference of functional principal component (FPC) scores remains underexplored. It is noted that FPC scores contain deeper information of functional data beyond mean, covariance, or eigenfunctions, as illustrated in Figure 1 with 100 trajectories from different distributions of FPC scores. This example highlights the inadequacy of basic descriptive statistics in fully capturing information in functional data, thus underscoring the need for developing estimation and inference methods for distributions of FPC scores.

In this paper, we consider discretely recorded data contaminated by measurement errors, which is motivated by the data applied in Section 6 and is also more relevant



(a) Left: normal, right: rescaled $t(3)$



(b) Left: uniform, right: Laplace

Figure 1: Random trajectories from different distributions of FPC scores with the same mean, covariance, and eigenfunctions.

to functional data from applied fields, such as Electroencephalogram (EEG) data and Electrocardiogram (ECG) data.

$$Y_{ij} = \eta_i \left(\frac{j}{N} \right) + \sigma \left(\frac{j}{N} \right) \varepsilon_{ij}, \quad i = 1, \dots, n, \quad j = 1, \dots, N. \quad (1.1)$$

Model (1.1) has been widely studied in the literature; see for instance Cao et al. (2012), Li and Yang (2022) and Zhong and Yang (2022). As emphasized in Hu and Li (2024), the observed grids $\{j/N\}_{j=1}^N$ in model (1.1) can be relaxed to vary over

subjects $\{x_{ij}\}_{i,j=1}^{n,N_i}$, as long as $\max_{1 \leq i \leq n, 1 \leq j \leq N_i-1} |x_{ij} - x_{i,j+1}| = \mathcal{O}(N^{-1})$. Also, the observation of grids can be random with positive density over $[0, 1]$. In these irregular scenarios, the main theoretical results can be proved similarly. The i.i.d. processes $\eta_i(x)$, $1 \leq i \leq n$, live in the space $L^2[0, 1]$ almost surely, satisfying $\mathbb{E} \int_0^1 \eta^2(x) dx < \infty$, with mean function $m(x) = \mathbb{E} \eta_i(x)$ and covariance function $G(x, x') = \text{Cov}(\eta_i(x), \eta_i(x'))$. The measurement errors ε_{ij} , $1 \leq i \leq n$, $1 \leq j \leq N$, are i.i.d. random variables with zero mean and unit variance and $\sigma^2(x)$ is the variance function. According to Mercer's lemma, the covariance function can be decomposed as $G(x, x') = \sum_{k=1}^{\infty} \lambda_k \psi_k(x) \psi_k(x')$, where $\{\lambda_k\}_{k=1}^{\infty}$ are a series of decreasing positive eigenvalues and $\{\psi_k(x)\}_{k=1}^{\infty}$ are the corresponding eigenfunctions, also called functional principal components (FPCs), which form an orthogonal basis of $L^2[0, 1]$ such that $\sum_{k=1}^{\infty} \lambda_k < \infty$ and $\int G(x, x') \psi_k(x') dx' = \lambda_k \psi_k(x)$. Then for any $1 \leq i \leq n$, the zero-mean process $\chi_i(x) = \eta_i(x) - m(x)$, $x \in [0, 1]$, allows general Karhunen-Loève representation $\chi_i(x) = \sum_{k=1}^{\infty} \xi_{ik} \phi_k(x)$, in which the rescaled eigenfunctions $\{\phi_k(x)\}_{k=1}^{\infty}$ satisfy that $\phi_k(x) = \sqrt{\lambda_k} \psi_k(x)$ and $\int \chi_i(x) \phi_k(x) dx = \lambda_k \xi_{ik}$ for $k \geq 1$. The random coefficients ξ_{ik} are uncorrelated over k , with mean 0 and variance 1, referred to as FPC scores.

Although the FPC scores are well-defined mathematical objects, they are unobservable to the data-handling statistician. It may also be difficult to accurately specify the distribution of FPC scores without any prior knowledge in the initial

stage of FPCA. Meanwhile, as far as we know, there do not exist any results on the distribution estimation of FPC scores. Therefore, developing estimation and statistical inference procedures for the CDF of FPC scores is of great interest. To achieve this, we first introduce a procedure for estimating FPC scores. We then propose a general approach for estimating the CDF of FPC scores, including a nonsmooth and a smooth estimator, and show that they are asymptotically equivalent. Afterwards, we novelly construct the simultaneous confidence bands (SCBs) for the CDF of FPC scores, which are powerful tools for quantifying the variability of complex functions and making global inference, as seen in the SCBs for probability density functions in Bickel and Rosenblatt (1973), for regression functions in Wang and Yang (2009), and for mean functions of functional data in Cao et al. (2012).

To proceed, it is also meaningful to test the “distribution” of functional data. Through the Karhunen-Loève representation, it is noted that the randomness of the demeaned random process $\chi_i(x)$ is completely determined by the distribution of FPC scores. Therefore, we can break down the testing procedure for infinite-dimensional objects into testing the distribution of scalar random variables, i.e. testing whether the distribution of FPC scores $F_k(\cdot)$ is some pre-specified distribution $F_k^*(\cdot)$. This testing problem can be formulated as the following high-dimensional hypothesis test,

as $\kappa_n \rightarrow \infty$ and $n \rightarrow \infty$,

$$H_0 : F_k(x) = F_k^*(x), 1 \leq k \leq \kappa_n, \text{ v.s. } H_1 : F_{k_0}(x) \neq F_{k_0}^*(x), \exists 1 \leq k_0 \leq \kappa_n. \quad (1.2)$$

In addition, the normality assumption is widely used in functional data analysis, which is the basic requirement of further theoretical results, see Yao et al. (2005a), Constantinou et al. (2017) and Hörmann et al. (2018), leading to the importance of test for the normality of functional data as a special case:

$$H_0 : F_k(x) = \Phi(x), 1 \leq k \leq \kappa_n, \text{ v.s. } H_1 : F_{k_0}(x) \neq \Phi(x), \exists 1 \leq k_0 \leq \kappa_n, \quad (1.3)$$

where $\Phi(x)$ is the CDF of standard normal random variables. The above hypothesis test problem (1.3) raised in Górecki et al. (2018) and Hörmann et al. (2022). Previous works on this topic often face greater technical difficulties and assume that functional data can be sufficiently well approximated by a projection onto a finite-dimensional subspace spanned by a few eigenfunctions. As a result, they consider only the first fixed p FPC scores; see Yao et al. (2005a), Berkes et al. (2009), Górecki et al. (2018), and Hörmann et al. (2022), or require the number of positive eigenvalues in the Karhunen-Loève expansion to be finite, limiting the scope of applicability; see Chen and Song (2015). However, in contrast to multivariate data, one major obstacle in the analysis of functional data is the infinite dimensionality of the data, which

also explains the intractability of the asymptotic distribution of L_2 -type statistics in functional data analysis. To reflect this, Fremdt et al. (2014) and Ghale-Joogh and Hosseini-Nasab (2018) propose procedures by considering the projections on subspaces spanned by an increasing number of FPCs. They point out that this approach allows to derive procedures which are fairly insensitive to the selection of the number of FPC scores used for inference. See also Liang et al. (2022) and Wang et al. (2022) more recently. Along this line, the number of FPC scores we focus on also diverges to infinity as the sample size increases in this paper, preserving the infinite-dimensional nature of functional data, and bringing many challenges in our methodological and theoretical developments. We propose a Kolmogorov-Smirnov type and a Cramér-von Mises type test statistic, which can handle principal components with a diverging number. Asymptotic properties are derived to show that the proposed procedures asymptotically control the type-I error at the nominal level, and power analysis is also investigated. Notably, our proposed method is not only able to address the problem of testing normality of functional data, but it is also applicable to testing whether the distribution of FPC scores is equal to any other given distributions in hypothesis (1.2). To the best of our knowledge, this is the first time that testing procedures for the distribution of FPC scores have been proposed.

The paper is structured as follows: Section 2 details the estimation method for FPC scores and their CDF. Section 3 presents the main theoretical results for

constructing SCBs and the test procedure for FPC score distribution. Section 4 covers the implementation of these methods. A numerical simulation study assessing the performance of these procedures is in Section 5, along with real data analysis of functional datasets and EEG data in Section 6. The final section offers conclusions and discussions. Supplementary material contains all proofs and additional tables and figures.

2. Methodology

2.1 Estimating the CDF of FPC scores

In this section, we present a method to recover FPC scores $\{\xi_{ik}\}_{i=1,k=1}^{n,\infty}$ and estimate their CDFs. For fully observed trajectories $\{\eta_i(x)\}_{i=1}^n$, moment-based estimators provide mean and covariance functions, $\tilde{m}(x) = n^{-1} \sum_{i=1}^n \eta_i(x)$, $\tilde{G}(x, x') = n^{-1} \sum_{i=1}^n (\eta_i(x) - \tilde{m}(x))(\eta_i(x') - \tilde{m}(x'))$ for $x, x' \in [0, 1]$. By solving the Fredholm equation $\int_0^1 \tilde{G}(x, x') \tilde{\psi}_k(x') dx' = \tilde{\lambda}_k \tilde{\psi}_k(x)$ for $k \in \mathbb{Z}_+$, we access the estimated eigen-systems $\{\tilde{\lambda}_k, \tilde{\psi}_k\}_{k \in \mathbb{Z}_+}$. The FPC scores ξ_{ik} 's are approximated using the plug-in estimator $\tilde{\xi}_{ik} = \tilde{\lambda}_k^{-1/2} \int_{\mathbb{R}} (\eta_i(x) - \tilde{m}(x)) \tilde{\psi}_k(x) dx$, and the empirical CDF is obtained as a nonsmooth estimator,

$$\tilde{F}_{nk}^\dagger(x) = \frac{1}{n} \sum_{i=1}^n I(\tilde{\xi}_{ik} \leq x), \quad x \in \mathbb{R}. \quad (2.4)$$

2.1 Estimating the CDF of FPC scores

To address the discontinuous nature of \tilde{F}_{nk}^\dagger , we introduce the kernel-based estimator $\tilde{F}_{nk}(x)$, defined as:

$$\tilde{F}_{nk}(x) = \frac{1}{n} \sum_{i=1}^n \int_{-\infty}^x K_h(u - \tilde{\xi}_{ik}) du, \quad x \in \mathbb{R}, \quad (2.5)$$

where $K_h(\cdot) = h^{-1}K(\cdot/h)$, with $K(\cdot)$ being a kernel function, and $h = h_n > 0$ is the so-called bandwidth. However, these estimators are infeasible, since only contaminated data $\{Y_{ij}\}_{i=1, j=1}^{n, N}$ are available. A practical solution is replacing $\eta_i(x)$ with a nonparametric smoother $\hat{\eta}_i(x)$, yielding feasible estimators for the mean and covariance function, i.e., for $x, x' \in [0, 1]$,

$$\hat{m}(x) = \frac{1}{n} \sum_{i=1}^n \hat{\eta}_i(x), \quad \hat{G}(x, x') = \frac{1}{n} \sum_{i=1}^n (\hat{\eta}_i(x) - \hat{m}(x)) (\hat{\eta}_i(x') - \hat{m}(x')). \quad (2.6)$$

We will provide further details on the construction of $\hat{\eta}_i(x)$ in Subsection 2.2. This leads to feasible estimators of eigensystems by solving

$$\int \hat{G}(x, x') \hat{\psi}_k(x') dx' = \hat{\lambda}_k \hat{\psi}_k(x), \quad x \in \mathbb{R}, \quad k \in \mathbb{Z}_+, \quad (2.7)$$

and recovering the FPC scores ξ_{ik} 's by $\hat{\xi}_{ik} = N^{-1} \sum_{j=1}^N \hat{\lambda}_k^{-1/2} (Y_{ij} - \hat{m}(j/N)) \hat{\psi}_k(j/N)$.

Hence, we replace the infeasible estimators $\tilde{\xi}_{ik}$'s by the feasible ones $\hat{\xi}_{ik}$'s to estimate the CDF of FPC scores in the estimators (2.4) and (2.5), and obtain the empirical

distribution function of $\{\widehat{\xi}_{ik}\}_{i=1}^n$ and kernel-based version, respectively,

$$\widehat{F}_{nk}^\dagger(x) = \frac{1}{n} \sum_{i=1}^n I(\widehat{\xi}_{ik} \leq x), \quad \widehat{F}_{nk}(x) = \frac{1}{n} \sum_{i=1}^n \int_{-\infty}^x K_h(u - \widehat{\xi}_{ik}) du, \quad x \in \mathbb{R}. \quad (2.8)$$

which are both accessible to data-handling statisticians. If $\widehat{\eta}_i(x)$ closely approximates $\eta_i(x)$, then \widehat{F}_{nk}^\dagger and \widehat{F}_{nk} should asymptotically behave like $\widetilde{F}_{nk}^\dagger$ and \widetilde{F}_{nk} , achieving oracle efficiency, as discussed in Section 3.

2.2 Recovering trajectories

We now introduce a convenient estimator for recovering trajectories. B-spline smoothing is recommended due to its computational efficiency explained below.

To describe it precisely, denote by $\{t_l\}_{l=1}^{N_s}$ a sequence of equally-spaced points. We call $t_l = l/(N_s + 1)$ for $l \in \{1, 2, \dots, N_s\}$ interior knots with $0 < t_1 < \dots < t_{N_s} < 1$, which divide the interval $[0, 1]$ into $N_s + 1$ equal subintervals $I_l = [t_l, t_{l+1})$ for $l = 0, 1, \dots, N_s - 1$ and $I_{N_s} = [t_{N_s}, 1]$. For any positive integer p , let $t_{1-p} = \dots = t_{-1} = 0$ and $t_{N_s+p} = \dots = t_{N_s+1} = 1$ be auxiliary knots. Let $\mathcal{S}^{(p-2)} = \mathcal{S}^{(p-2)}[0, 1]$ denote the polynomial spline space of order p on I_l for $l \in \{0, \dots, N_s\}$, which consists of all $(p - 2)$ times continuously differentiable functions on $[0, 1]$ that are polynomials of degree $(p - 1)$ on subintervals I_l for $l \in \{0, \dots, N_s\}$. Then, we denote by $\{B_{l,p}(\cdot), 1 \leq l \leq N_s + p\}$ the p th-order B-spline basis functions of $\mathcal{S}^{(p-2)}$. Hence,

$\mathcal{S}^{(p-2)} = \{\sum_{l=1}^{N_s+p} a_{l,p} B_{l,p}(\cdot) : a_{l,p} \in \mathbb{R}\}$; see De Boor (1978) for more details.

The individual unknown trajectory $\eta_i(x)$ could be estimated via B-spline as $\hat{\eta}_i(\cdot) := \arg \min_{g_i \in \mathcal{S}^{(p-2)}} \sum_{j=1}^N (Y_{ij} - g_i(j/N))^2$ for $1 \leq i \leq n$. To further simplify the forms of $\{\hat{\lambda}_k, \hat{\psi}_k\}_{k \in \mathbb{Z}_+}$ and reduce the computational burden of solving (2.7) via discretization and high-dimensional matrix spectral decomposition, one can write:

$\hat{\eta}_i(x) := \sum_{l=1}^{N_s+p} \hat{\beta}_{i,l,p} B_{l,p}(x)$, $1 \leq i \leq n$, where

$$\{\hat{\beta}_{i,1,p}, \dots, \hat{\beta}_{i,N_s+p,p}\}^\top = \arg \min_{\{\beta_{i,1,p}, \dots, \beta_{i,N_s+p,p}\}^\top \in \mathbb{R}^{N_s+p}} \sum_{j=1}^N \left\{ Y_{ij} - \sum_{l=1}^{N_s+p} \beta_{i,l,p} B_{l,p}(j/N) \right\}.$$

Therefore, one has the following B-spline representation of covariance estimation

$\hat{G}(x, x') = \sum_{l=1}^{N_s+p} \sum_{l'=1}^{N_s+p} \hat{\beta}_{l,l'} B_{l,p}(x) B_{l',p}(x')$, where

$$\hat{\beta}_{l,l'} = \frac{1}{n} \sum_{i=1}^n \left\{ \left(\hat{\beta}_{i,l,p} - \frac{1}{n} \sum_{j=1}^n \hat{\beta}_{j,l,p} \right) \left(\hat{\beta}_{i,l',p} - \frac{1}{n} \sum_{j=1}^n \hat{\beta}_{j,l',p} \right) \right\}, \quad 1 \leq l, l' \leq N_s + p,$$

are the coefficients. Similarly, one considers spline approximation of $\hat{\psi}(x)$ in (2.7), i.e.,

$\hat{\psi}_k(x) = \sum_{l=1}^{N_s+p} \hat{\gamma}_{l,k} B_{l,p}(x)$, in which $\hat{\gamma}_{l,k}$'s are coefficients determined by $N^{-1} \hat{\beta} \mathbf{B}^\top \mathbf{B} \hat{\gamma}_k =$

$\hat{\lambda}_k \hat{\gamma}_k$ subject to $N^{-1} \hat{\gamma}_k^\top \mathbf{B}^\top \mathbf{B} \hat{\gamma}_k = 1$ with $\hat{\gamma}_k = (\hat{\gamma}_{1,k}, \dots, \hat{\gamma}_{N_s+p,k})^\top$, $\hat{\beta} = \{\hat{\beta}_{l,l'}\}_{l,l'=1}^{N_s+p}$

and $\mathbf{B} = \{B_{l,p}(j/N)\}_{l,j=1}^{N_s+p,N}$. The Cholesky decomposition $N^{-1} \mathbf{B}^\top \mathbf{B} = \mathbf{L}_B \mathbf{L}_B^\top$ allows

us to rewrite the solution of (2.7) as the eigenvalues and unit eigenvectors of $\mathbf{L}_B^\top \hat{\beta} \mathbf{L}_B$.

Specifically, for each $k \in \mathbb{Z}_+$, we have that $\mathbf{L}_B^\top \hat{\beta} \mathbf{L}_B \mathbf{L}_B^\top \hat{\gamma}_k = \hat{\lambda}_k \mathbf{L}_B^\top \hat{\gamma}_k$. This means that

$\widehat{\lambda}_k$ and $\mathbf{L}_B^\top \widehat{\gamma}_k$ are the eigenvalues and unit eigenvectors of $\mathbf{L}_B^\top \widehat{\boldsymbol{\beta}} \mathbf{L}_B$, respectively. To obtain $\widehat{\gamma}_k$, we multiply $(\mathbf{L}_B^\top)^{-1}$ to the unit eigenvectors of $\mathbf{L}_B^\top \widehat{\boldsymbol{\beta}} \mathbf{L}_B$. Then, we calculate $\widehat{\psi}_k(x)$ and $\widehat{\phi}_k(x) = \widehat{\lambda}_k^{1/2} \widehat{\psi}_k(x)$. It is worth noting that this estimation procedure only involves solving for the eigenvalues of $(N_s + p) \times (N_s + p)$ dimensional matrices, rather than $N \times N$ dimensional matrices. This significantly speeds up the computational process, as the order of N_s is usually much smaller than N .

3. Asymptotic properties

Throughout the paper, for sequences a_n and b_n , denote $a_n \asymp b_n$ if there exist positive constants c and C such that $cb_n \leq a_n \leq Cb_n$. For real numbers a and b , the notation $a \wedge b$ denotes $\min\{a, b\}$. The notation $\xrightarrow{\mathbb{P}}$ denotes convergence in probability. For a non-negative integer q and a real number $\mu \in (0, 1]$, we define $\mathcal{H}^{(q, \mu)}(\Omega)$ as the space of (q, μ) -Hölder continuous functions on domain Ω , that is,

$$\mathcal{H}^{(q, \mu)}(\Omega) = \left\{ h : \Omega \rightarrow \mathbb{R} \left| \|h\|_{q, \mu} = \sup_{x, y \in \Omega, x \neq y} \frac{|h^{(q)}(x) - h^{(q)}(y)|}{|x - y|^\mu} < \infty \right. \right\}$$

To investigate the asymptotic properties of $\widehat{F}_{nk}(x)$ and \widehat{F}_{nk}^\dagger , some assumptions are imposed first.

(A1) For any small positive number ϱ , the nonparametric estimator $\widehat{\eta}_i(x)$ satisfies that, as $n \rightarrow \infty$, $\|\widehat{m} - \widetilde{m}\|_\infty = o_p(n^{-1/2})$ and $\|\widehat{G} - \widetilde{G}\|_\infty = \mathcal{O}_p(n^{-1/2-\varrho})$,

where \hat{m} and \hat{G} are defined in (2.6).

(A2) The non-zero eigenvalues λ_j are distinct and have a polynomial decay rate, i.e.

$\lambda_j \asymp j^{-\tau}$ for $1 \leq j \leq \kappa_n$, $\tau > 1$, and κ_n satisfies that $\kappa_n = \mathcal{O}(\log n)$.

(A3) The CDF of k -th FPC score $F_k(\cdot) \in \mathcal{H}^{(1,1)}(\mathbb{R})$ such that $\sup_k \|F_k\|_{1,1} < \infty$,

$\sup_k \|f_k\|_\infty < \infty$. In addition, $g_k(x) = x f_k(x) \in \mathcal{H}^{(0,\nu_1)}(\mathbb{R})$ with $\nu_1 \in (0, 1]$,

satisfying $\sup_k \|g_k\|_{0,\nu_1} < \infty$, $\sup_k \|g_k\|_\infty < \infty$.

(A4) $n = \mathcal{O}(N^\theta)$ for some constant $\theta \in (0, 1]$, and $n = n(N) \rightarrow \infty$ as $N \rightarrow \infty$.

(A5) $\sum_{k=1}^\infty \|\phi_k\|_\infty < \infty$ and $\sum_{k=1}^\infty \|\phi_k\|_{0,\varpi} < \infty$ for some constant $\varpi \in (\theta/2, 1]$.

(A6) The FPC scores $\{\xi_{ik}\}_{i \geq 1, k \geq 1}$, which are independent over $k \geq 1$ and i.i.d. over

$i \geq 1$, satisfy $\sup_k \mathbb{E} |\xi_{1k}|^{r_1} < \infty$ with $r_1 > \max\{2\theta/(2\varpi - \theta), 8\}$. $\{\varepsilon_{ij}\}_{i \geq 1, j \geq 1}$ are

i.i.d. and independent of the FPC scores, with $\mathbb{E} |\varepsilon_{11}|^{r_2} < \infty$ and $r_2 > 4 + 2\theta$.

(A7) The kernel function $K(\cdot)$ for $\hat{F}_{nk}(\cdot)$ is twice continuously differentiable, with

bandwidth $h = h_n$ satisfying $h \asymp n^{-t_1}$ and $1/4 < t_1 < \min\{(r_1 - 4)/(2r_1), 1/3\}$

as $n \rightarrow \infty$. The kernel function $L(\cdot)$ in (4.13) for density estimation has

bounded derivative, with bandwidth $H = H_n$ satisfying $H \asymp n^{-t_2}$ and $1/8 <$

$t_2 < 1/4 - 1/(2r_1)$ as $n \rightarrow \infty$. Both kernel functions are symmetric probability

density functions supported on $[-1, 1]$.

Our assumptions (A1)-(A7) are standard and commonly satisfied. (A1) is fundamental for nonparametric estimators and supports pre-smoothing techniques like kernel smoothing, wavelets, and B-splines. (A2) controls the decay of eigenvalues and the growth rate of FPC scores, crucial for simultaneous inference (Cai and Hall (2006)). (A3) ensures the smoothness of CDF $F_k(\cdot)$. (A4) requires sufficient data density, with n observations on N grids. (A5) focuses on the boundedness and continuity of FPCs. To ensure (A2) and (A5) hold simultaneously, we provide an example by considering $\{\psi_k\}_{k=1}^\infty$ being Fourier basis with $\tau > 2(\varpi + 1) > \theta + 2$, for instance, $\tau = 4$. (A6) includes moment conditions and assumes independence between FPC scores ξ_{ik} and measurement errors ε_{ij} . This independence is key for the joint asymptotic properties of \widehat{F}_{nk}^\dagger and \widehat{F}_{nk} as $\kappa_n \rightarrow \infty$. However, in non-Gaussian processes where the distribution of data depends on the joint distributions of FPC scores, this assumption needs to be relaxed. Nevertheless, estimating the multivariate distribution in such cases poses a significant challenge. While we introduce the first inference procedure for FPC scores with an increasing number of components, addressing high-dimensional multivariate distribution estimation lies outside the scope of this work. (A7) about kernels $K(\cdot)$ and $L(\cdot)$ is common in literature (Wang et al. (2014)).

Remark 1. Assumption (A4) implies an upper limit on θ of $\theta \leq 1$, suggesting that the number of grids N within each trajectory should not significantly lag behind the sample size n . This contrasts with the sparse setting; see Yao et al. (2005a), Li

and Hsing (2010) and Zhang and Li (2021), where the number of each trajectory's observation has a finite expectation, aggregating all observations is necessary to estimate eigensystems and FPC scores, resulting in significantly different asymptotic results, which is beyond the scope of this paper.

Below, we will present some high-level assumptions under Assumption (A2) - (A7) to satisfy Assumption (A1), ensuring that our general methodology applies at least to the B-spline approach.

(B1) There exist an integer $q > 0$ and a constant $\mu \in (0, 1]$, such that the mean function $m(\cdot) \in \mathcal{H}^{(q,\mu)}[0, 1]$. In the following, we denote $p^* = q + \mu$.

(B2) The standard deviation function $\sigma(\cdot) \in \mathcal{H}^{(0,\nu_2)}[0, 1]$ for positive index $\nu_2 \in (0, 1]$.

(B3) The demeaned trajectory $\chi_i(\cdot) \in \mathcal{H}^{(q,\mu)}[0, 1]$ almost surely with $\mathbb{E} \|\chi_i\|_{q,\mu}^{r_1} < \infty$ for q, μ in (B1) and r_1 in (A6), and there exist increasing positive integers $\{k_n\}_{n=1}^\infty$ such that $k_n = \mathcal{O}(n^{\omega_1})$ for some $\omega_1 > 0$ and the small positive number ϱ mentioned in (A1), as $n \rightarrow \infty$, $\sum_{k=k_n+1}^\infty \|\phi_k\|_\infty = \mathcal{O}(n^{-1/2-\varrho})$.

(B4) The number of interior knots $N_s \asymp N^\iota d_N$ for some $\iota > 0$ with $d_N + d_N^{-1} = \mathcal{O}(\log^\iota N)$ as $N \rightarrow \infty$. For θ in (A4), r_1, r_2 in (A6), p^* in (B1), ν_2 in (B2), ω_1 in (B3), the spline order $p \geq p^*$, $r_1 > 4 + 2\omega_1$, and

$$\max \left\{ \frac{\theta}{p^*} \left(\frac{4}{r_1} + \frac{1}{2} \right), 1 - \nu_2 \right\} < \gamma < 1 - \frac{\theta + 2}{r_2} - \theta \left(\frac{\omega_1 + 2}{r_1} + \frac{1}{2} \right).$$

In fact, these assumptions are fairly mild. (B1) - (B3) ensure the smoothness of the mean function, the covariance function, and the FPCs. The range of parameters specified in (A4), (A6), and (B1) - (B3) is given in (B4). A reasonable choice of parameters in (B4) is $q + \mu = p^* = 4$, $\nu = 1$, $\theta = 1$, $p = 4$ (cubic spline), $\gamma = 1/4$, and $d_N \asymp \log \log N$. These constants are used as default values for implementation.

To begin with, we introduce the asymptotic linear expansion and the weak convergence result about the infeasible estimator \tilde{F}_{nk} in (2.4). Denote $\zeta_{nk}(x) := n^{-1} \sum_{i=1}^n \{I(\xi_{ik} \leq x) - F_k(x) + \xi_{ik} f_k(x) + x f_k(x) (\xi_{ik}^2 - 1) / 2\}$.

Theorem 1. *Under Assumptions (A3) and (A5) - (A7), for any $k \in \mathbb{Z}_+$, as $n \rightarrow \infty$, $\sup_{x \in \mathbb{R}} \sqrt{n} \left| \tilde{F}_{nk}(x) - F_k(x) - \zeta_{nk}(x) \right| = o_p(1)$. Then, one has $\sqrt{n} \left(\tilde{F}_{nk}(x) - F_k(x) \right) \xrightarrow{d} \zeta_k(x)$, in the Skorokhod space $D(-\infty, \infty)$, where $\zeta_k(x)$ is a Gaussian process with mean zero and covariance function*

$$\begin{aligned} \Sigma_k(x, y) &= F_k(x \wedge y) - F_k(x)F_k(y) + f_k(x)f_k(y) + f_k(x)\mathbb{E}(\xi_{ik}I(\xi_{ik} \leq y)) \\ &+ f_k(y)\mathbb{E}(\xi_{ik}I(\xi_{ik} \leq x)) + \frac{1}{4}(\mathbb{E}\xi_{ik}^4 - 1)xyf_k(x)f_k(y) + \frac{1}{2}xf_k(x)\mathbb{E}((\xi_{ik}^2 - 1)I(\xi_{ik} \leq y)) \\ &+ \frac{1}{2}yf_k(y)\mathbb{E}((\xi_{ik}^2 - 1)I(\xi_{ik} \leq x)) + \frac{1}{2}xf_k(x)f_k(y)\mathbb{E}\xi_{ik}^3 + \frac{1}{2}yf_k(y)f_k(x)\mathbb{E}\xi_{ik}^3, \quad x, y \in \mathbb{R}. \end{aligned}$$

Remark 2. Theorem 1 provides that \tilde{F}_{nk} is asymptotically equivalent to F_k plus some correction terms $n^{-1} \sum_{i=1}^n \xi_{ik} f_k(x)$ and $(2n)^{-1} \sum_{i=1}^n (\xi_{ik}^2 - 1) x f_k(x)$, which arise due to the estimation errors of \tilde{m} and $\tilde{\lambda}_k$ in $\tilde{\xi}_{ik}$ defined in section 2.1, respectively. It

is interesting to note that the estimation error of $\tilde{\psi}_k$ did not introduce any correction terms, as the asymptotic expansion of $\tilde{\psi}_k$ degenerated after kernel smoothing. Similar theoretical results can be found in Neumeyer and Van Keilegom (2010), which discusses estimation of the distribution of the standardized measurement error after detrending in nonparametric regression. The role of \tilde{m} and $\tilde{\lambda}_k$ in $\tilde{\xi}_{ik}$ can be analogously compared to detrending and standardization, and $\Sigma_k(\cdot, \cdot)$ is the covariance function of process $\sqrt{n}\zeta_{nk}(\cdot)$.

Next, the gap between the infeasible estimator \tilde{F}_{nk} in (2.4) and the feasible estimator \hat{F}_{nk} in (2.8) is compensated by the following theorem.

Theorem 2. *Under Assumptions (A1) - (A7), as $n \rightarrow \infty$, one has that*

$$\max_{1 \leq k \leq \kappa_n} \sup_{x \in \mathbb{R}} \sqrt{n} \left| \tilde{F}_{nk}(x) - \hat{F}_{nk}(x) \right| = o_p(1).$$

Theorem 2 establishes that the proposed smooth estimator \hat{F}_{nk} has oracle efficiency, meaning that the cost of using \hat{F}_{nk} instead of \tilde{F}_{nk} is asymptotically negligible up to order $n^{-1/2}$. Therefore, the proposed estimators \hat{F}_{nk} have the same asymptotic property as \tilde{F}_{nk} in Theorem 1. This leads to the following Theorem 3, which enables us to derive the smooth SCB of F_k in Section 4.2.

Theorem 3. *Under Assumptions (A1) and (A3) - (A7), for any $k \in \mathbb{Z}_+$, as $n \rightarrow \infty$,*

$$\sup_{t \in \mathbb{R}} \left| \mathbb{P} \left(\sup_{x \in \mathbb{R}} \sqrt{n} \left| \hat{F}_{nk}(x) - F_k(x) \right| \leq t \right) - \mathbb{P} \left(\sup_{x \in \mathbb{R}} |\zeta_k(x)| \leq t \right) \right| = o(1).$$

It is then of great interest to test all κ_n hypothesis (1.2) simultaneously, which is useful for identifying important features in functional data. We consider the following goodness fits tests, including Kolmogorov-Smirnov (KS) type test statistic S_n and Cramér-von Mises (CVM) type test statistic V_n as

$$S_n = \max_{1 \leq k \leq \kappa_n} \sup_{x \in \mathbb{R}} \sqrt{n} \left| \widehat{F}_{nk}(x) - F_k^*(x) \right|, \quad V_n = \sum_{k=1}^{\kappa_n} \widehat{\lambda}_k \int_{\mathbb{R}} n \left(\widehat{F}_{nk}(x) - F_k^*(x) \right)^2 dx.$$

The two statistics under consideration are designed for testing differences in CDFs in different ways. The KS-type statistic emphasizes the maximum difference between the distributions and considers all FPC scores to be equally important for testing. The CVM-type statistic, on the other hand, focuses on the cumulative difference between the distributions and uses the eigenvalues as weights to assess the significance of the FPC scores. They have the same asymptotic size and power, which are stated in Theorem 4 and Proposition 3 below, but they may yield different results with finite sample sizes, depending on the user's priorities about the null hypothesis (1.2).

Theorem 4. *Under Assumptions (A1) - (A7) and the null H_0 in (1.2), there exist independent Gaussian processes $\{\zeta_k(\cdot)\}_{k=1}^{\kappa_n}$, where $\zeta_k(\cdot)$ is mean zero and has the covariance function $\Sigma_k(\cdot, \cdot)$ such that, under null hypothesis, as $n \rightarrow \infty$,*

$$\sup_{t \in \mathbb{R}} \left| \mathbb{P}(S_n \leq t) - \mathbb{P} \left(\max_{1 \leq k \leq \kappa_n} \sup_{x \in \mathbb{R}} |\zeta_k(x)| \leq t \right) \right| \rightarrow 0,$$

$$\sup_{t \in \mathbb{R}} \left| \mathbb{P}(V_n \leq t) - \mathbb{P} \left(\sum_{k=1}^{\kappa_n} \lambda_k \int_{\mathbb{R}} \zeta_k^2(x) dx \leq t \right) \right| \rightarrow 0.$$

Theorem 4 provides the approximate distribution of S_n and V_n through the supremum-norm and weighted L_2 -norm of Gaussian processes $\{\zeta_k(\cdot)\}_{k=1}^{\kappa_n}$ under the null H_0 in (1.2). If the covariance function $\{\Sigma_k(\cdot, \cdot)\}_{k=1}^{\kappa_n}$ were known, these two distributions could be easily simulated. We will discuss a uniformly consistent estimator for $\{\Sigma_k(\cdot, \cdot)\}_{k=1}^{\kappa_n}$ and show the consistency of the proposed testing procedures in Section 4.

To bridge the gap between the infeasible estimators \tilde{F}_{nk} and \tilde{F}_{nk}^\dagger , and between the feasible estimators \hat{F}_{nk} and \hat{F}_{nk}^\dagger , we introduce Proposition 1.

Proposition 1. *Under Assumptions (A1) - (A7), as $n \rightarrow \infty$, one has that*

$$\max_{1 \leq k \leq \kappa_n} \sup_{x \in \mathbb{R}} \sqrt{n} \left(\left| \tilde{F}_{nk}(x) - \tilde{F}_{nk}^\dagger(x) \right| + \left| \hat{F}_{nk}(x) - \hat{F}_{nk}^\dagger(x) \right| \right) = o_p(1).$$

Proposition 1 shows that the cost of using the proposed nonsmooth estimators \hat{F}_{nk}^\dagger instead of \hat{F}_{nk} is also uniformly asymptotically indistinguishable up to order $n^{-1/2}$. Combined with Theorem 2, this implies that the nonsmooth estimator \hat{F}_{nk}^\dagger also has oracle efficiency. In other words, the proposed estimators \hat{F}_{nk}^\dagger and \hat{F}_{nk} have the same asymptotic properties as the infeasible estimators \tilde{F}_{nk}^\dagger and \tilde{F}_{nk} . Therefore, we can use the nonsmooth estimator \hat{F}_{nk}^\dagger to obtain the following result.

Theorem 5. *Under the same conditions in Theorem 3 and Theorem 4, the state-*

ments in Theorem 3 and Theorem 4 still hold respectively, after replacing \widehat{F}_{nk} by \widehat{F}_{nk}^\dagger .

The corresponding test statistics for (1.2) become S_n^\dagger and V_n^\dagger respectively,

$$S_n^\dagger = \max_{1 \leq k \leq \kappa_n} \sup_{x \in \mathbb{R}} \sqrt{n} \left| \widehat{F}_{nk}^\dagger(x) - F_k^*(x) \right|, \quad V_n^\dagger = \sum_{k=1}^{\kappa_n} \widehat{\lambda}_k \int_{\mathbb{R}} n \left(\widehat{F}_{nk}^\dagger(x) - F_k^*(x) \right)^2 dx.$$

Hence, statistical inference can be performed with either \widehat{F}_{nk} or \widehat{F}_{nk}^\dagger , such as constructing SCBs of F_k , and performing uniform hypothesis testing for $\{F_k\}_{k=1}^{\kappa_n}$.

The implementation details and the power analysis will be described in Section 4.

In addition to one-sample problems, sometimes two-sample problems are also full of interest. For example, certain physiological data of people, such as height, weight, etc., have different means and variances between males and females, but may indeed belong to the same family of distributions, as illustrated in Section 6, which leads us to consider the hypothesis in (1.2) can be extended to a two-sample problem. For processes $\{\eta_i^{(s)}(x)\}_{i=1}^{n^{(s)}}$ defined on $[0, 1]$, $s = 1, 2$, with mean functions $m_s(x)$, covariance functions $G_s(x, x')$, eigensystems $\{\lambda_{sk}, \psi_{sk}(x)\}_{k \in \mathbb{Z}_+}$, FPC scores $\{\xi_{ik}^{(s)}\}_{k \in \mathbb{Z}_+}$ with CDFs $\{F_{sk}(x)\}_{k \in \mathbb{Z}_+}$, variance functions $\sigma_s^2(x)$, and measurement errors $\varepsilon_{ij}^{(s)}$'s with zero mean and unit variance. Then, (1.2) is generalized to

$$H_0 : F_{1k}(x) = F_{2k}(x), 1 \leq k \leq \kappa_n^*, \text{ v.s. } H_1 : F_{1k}(x) \neq F_{2k}(x), \exists 1 \leq k_0 \leq \kappa_n^*, \quad (3.9)$$

which can be used to test whether the distributions of FPC scores of $\{\eta_i^{(s)}(x)\}_{i=1}^{n^{(s)}}$,

$s = 1, 2$, are the same. For the collected data

$$Y_{ij}^{(s)} = \eta_i^{(s)} \left(\frac{j}{N^{(s)}} \right) + \sigma_s \left(\frac{j}{N^{(s)}} \right) \varepsilon_{ij}^{(s)}, \quad 1 \leq i \leq n^{(s)}, \quad 1 \leq j \leq N^{(s)}. \quad (3.10)$$

Denote the ratio of two-sample sizes as $\hat{r} = n^{(1)}/n^{(2)}$, and assume that $r = \lim_{n^{(1)} \rightarrow \infty} n^{(1)}/n^{(2)}$ exists and is positive. Applying the estimators in (2.8), one obtains $\widehat{F}_{s,nk}$ or $\widehat{F}_{s,nk}^\dagger$ for $s = 1, 2$, and constructs the following KS-type or CVM-type statistics with $\kappa_n^* = \mathcal{O}(\log n^{(1)})$.

$$\begin{aligned} S_n^\circ &= \max_{1 \leq k \leq \kappa_n^*} \sup_{x \in \mathbb{R}} \sqrt{n^{(1)}} \left| \widehat{F}_{1,nk}(x) - \widehat{F}_{2,nk}(x) \right|, \\ S_n^\dagger &= \max_{1 \leq k \leq \kappa_n^*} \sup_{x \in \mathbb{R}} \sqrt{n^{(1)}} \left| \widehat{F}_{1,nk}^\dagger(x) - \widehat{F}_{2,nk}^\dagger(x) \right|, \\ V_n^\circ &= \sum_{k=1}^{\kappa_n^*} \left(\widehat{\lambda}_{1k} + \sqrt{\widehat{r}} \widehat{\lambda}_{2k} \right) \int_{\mathbb{R}} n^{(1)} \left(\widehat{F}_{1,nk}(x) - \widehat{F}_{2,nk}(x) \right)^2 dx, \\ V_n^\dagger &= \sum_{k=1}^{\kappa_n^*} \left(\widehat{\lambda}_{1k} + \sqrt{\widehat{r}} \widehat{\lambda}_{2k} \right) \int_{\mathbb{R}} n^{(1)} \left(\widehat{F}_{1,nk}^\dagger(x) - \widehat{F}_{2,nk}^\dagger(x) \right)^2 dx. \end{aligned}$$

Let $\{\zeta_{sk}(x)\}_{k=1}^{\kappa_n^*}$ be mutual independent Gaussian process for $s = 1, 2$, with mean zero and covariance function

$$\begin{aligned} \Sigma_{sk}(x, y) &= F_{sk}(x \wedge y) - F_{sk}(x)F_{sk}(y) + f_{sk}(x)f_{sk}(y) + f_{sk}(x)\mathbb{E} \left(\xi_{ik}^{(s)} I \left(\xi_{ik}^{(s)} \leq y \right) \right) \\ &+ f_{sk}(y)\mathbb{E} \left(\xi_{ik}^{(s)} I \left(\xi_{ik}^{(s)} \leq x \right) \right) + \frac{1}{4} \left(\mathbb{E}(\xi_{ik}^{(s)})^4 - 1 \right) xy f_{sk}(x) f_{sk}(y) \end{aligned}$$

$$\begin{aligned}
 & + \frac{1}{2} x f_{sk}(x) \mathbb{E} \left(((\xi_{ik}^{(s)})^2 - 1) I \left(\xi_{ik}^{(s)} \leq y \right) \right) + \frac{1}{2} y f_{sk}(y) \mathbb{E} \left(((\xi_{ik}^{(s)})^2 - 1) I \left(\xi_{ik}^{(s)} \leq x \right) \right) \\
 & + \frac{1}{2} x f_{sk}(x) f_{sk}(y) \mathbb{E} (\xi_{ik}^{(s)})^3 + \frac{1}{2} y f_{sk}(y) f_{sk}(x) \mathbb{E} (\xi_{ik}^{(s)})^3, \quad x, y \in \mathbb{R}.
 \end{aligned}$$

We mimic the two-sample t-test and state the following theorem whose proof is analogous to that of Theorems 4 and 5.

Theorem 6. *If Assumptions (A1) - (A7) are satisfied for the data $\{Y_{ij}^{(s)}\}$, $s = 1, 2$, respectively, under the null hypothesis in (3.9), as $n^{(1)} \rightarrow \infty$, we have the following*

$$\begin{aligned}
 & \sup_{t \in \mathbb{R}} \left| \mathbb{P} (S_n^\circ \leq t) - \mathbb{P} \left(\max_{1 \leq k \leq \kappa_n^*} \sup_{x \in \mathbb{R}} |\zeta_{1k}(x) + \sqrt{r} \zeta_{2k}(x)| \leq t \right) \right| \rightarrow 0, \\
 & \sup_{t \in \mathbb{R}} \left| \mathbb{P} (S_n^\dagger \leq t) - \mathbb{P} \left(\max_{1 \leq k \leq \kappa_n^*} \sup_{x \in \mathbb{R}} |\zeta_{1k}(x) + \sqrt{r} \zeta_{2k}(x)| \leq t \right) \right| \rightarrow 0, \\
 & \sup_{t \in \mathbb{R}} \left| \mathbb{P} (V_n^\circ \leq t) - \mathbb{P} \left(\sum_{k=1}^{\kappa_n^*} (\lambda_{1k} + \sqrt{r} \lambda_{2k}) \int_{\mathbb{R}} |\zeta_{1k}(x) + \sqrt{r} \zeta_{2k}(x)|^2 dx \leq t \right) \right| \rightarrow 0, \\
 & \sup_{t \in \mathbb{R}} \left| \mathbb{P} (V_n^\dagger \leq t) - \mathbb{P} \left(\sum_{k=1}^{\kappa_n^*} (\lambda_{1k} + \sqrt{r} \lambda_{2k}) \int_{\mathbb{R}} |\zeta_{1k}(x) + \sqrt{r} \zeta_{2k}(x)|^2 dx \leq t \right) \right| \rightarrow 0.
 \end{aligned}$$

4. Implementation

4.1 The selection of tuning parameters

A default setting of parameters was mentioned in Section 3, namely $q + \mu = p^* = 4$, $\nu = 1$, $\theta = 1$, $p = 4$, and $\gamma = 1/4$. The number of knots N_s is an important smoothing parameter, and we recommend using a data-driven method that minimizes the AIC

4.1 The selection of tuning parameters

value corresponding to $N_s \in [0.5N^{1/4}, 4N^{1/4}]$. The AIC value is defined as:

$$\text{AIC}(N_s) = \log \left\{ (nN)^{-1} \sum_{i=1}^n \sum_{j=1}^N (Y_{ij} - \hat{\eta}_i(j/N))^2 \right\} + \frac{8 + 2N_s}{N}. \quad (4.11)$$

For each trajectory, the number of knots can also be determined individually by replacing $(nN)^{-1} \sum_{i=1}^n \sum_{j=1}^N (Y_{ij} - \hat{\eta}_i(j/N))^2$ with $N^{-1} \sum_{j=1}^N (Y_{ij} - \hat{\eta}_i(j/N))^2$ in (4.11). However, we prefer to select a uniform N_s since we have assumed that $\{\eta_i\}_{i=1}^n$ is an i.i.d. process, which is more computationally convenient.

According to Assumption (A7), the smooth estimator \hat{F}_{nk} is computed using the triweight kernel $K(u) = 35(1 - u^2)^3/32$, for $|u| \leq 1$, and a bandwidth of $h = \text{IQR}n^{-1/4}/\log n$, where IQR denotes the sample interquartile range of the estimated FPC scores $\{\hat{\xi}_{ik}\}_{i=1}^n$. As for the kernel density estimator \hat{f}_k defined below in (4.13), we use the biweight kernel $L(u) = 15(1 - u^2)^2/16$, for $|u| \leq 1$, with the bandwidth $H = \text{IQR}n^{-1/6}$ as a rule of thumb, to satisfy Assumption (A7). In addition, based on Assumption (A2), the increasing number κ_n is chosen by the following empirically standard and efficient criteria, that is $\kappa_n = \min \left\{ N_s + p, \max \left\{ \arg \min_{1 \leq v \leq T} \left\{ \sum_{k=1}^v \hat{\lambda}_k / \sum_{k=1}^T \hat{\lambda}_k > 0.95 \right\}, \lceil \log n \rceil \right\} \right\}$, where $\{\hat{\lambda}_k\}_{k=1}^T$ are the first T estimated positive eigenvalues.

4.2 SCBs for the distribution of FPC scores

As stated in Theorem 3 and Theorem 5, the weak convergence of the proposed smooth estimator \widehat{F}_{nk} and nonsmooth estimator \widehat{F}_{nk}^\dagger is related to the Gaussian process $\zeta_k(\cdot)$ with covariance function $\Sigma_k(\cdot, \cdot)$. It is difficult to analytically derive the distribution of $\sup_{x \in [0,1]} |\zeta_k(x)|$ and calculate its quantile, as some quantities in the covariance function are unknown and need to be estimated. To estimate the quantile, for any fixed k , we define

$$\widehat{\Xi}_{ik}(x) = I(\widehat{\xi}_{ik} \leq x) - \widehat{F}_{nk}^\dagger(x) + \widehat{f}_k(x)\widehat{\xi}_{ik} + x\widehat{f}_k(x)\frac{\widehat{\xi}_{ik}^2 - 1}{2}, \quad (4.12)$$

$$\widehat{f}_k(x) := \frac{1}{n} \sum_{l=1}^n L_H(\widehat{\xi}_{lk} - x). \quad (4.13)$$

Further define the covariance estimator $\widehat{\Sigma}_k(s, t) = n^{-1} \sum_{i=1}^n \widehat{\Xi}_{ik}(s)\widehat{\Xi}_{ik}(t)$. The following Proposition 2 ensures that the covariance estimator $\widehat{\Sigma}_k(s, t)$ is uniformly convergent to the Gaussian covariance function $\Sigma_k(s, t)$.

Proposition 2. *Under Assumptions (A1) - (A7), as $n \rightarrow \infty$, one has that*

$$\max_{1 \leq k \leq \kappa_n} \sup_{(s,t) \in \mathbb{R}^2} \left| \widehat{\Sigma}_k(s, t) - \Sigma_k(s, t) \right| = \mathcal{O}_p(1).$$

Using the definition in (4.12), we construct random vectors $\left\{ \widehat{\Xi}_{ik}(z_l) \right\}_{l=1}^L$ for $1 \leq i \leq n$, allowing the computation of the sample covariance $\widehat{\Sigma}_k(\cdot, \cdot)$. Here, $z_1 < z_2 < \dots < z_L$ are L equally spaced grid points, with $\min_{i=1}^n \widehat{\xi}_{ik} = z_1$, $\max_{i=1}^n \widehat{\xi}_{ik} = z_M$, and L being a large integer. To estimate the upper α quantile of the maximal

4.3 Uniform testing for FPC scores

absolute value, we generate L -dimensional Gaussian vectors with zero mean and covariance matrix $\left\{ \widehat{\Sigma}_k(z_l, z_{l'}) \right\}_{l, l'=1}^L$ B times (where B is large). The empirical upper α quantile, $\widehat{Q}_{1-\alpha}$, is computed for each replication, with default $L = 101$ and $B = 1000$. Denote by $Q_{1-\alpha}$ the upper- α quantile of the distribution of $\sup_{x \in \mathbb{R}} |\zeta_k(x)|$, i.e., $\mathbb{P}(\sup_{x \in \mathbb{R}} |\zeta_k(x)| \leq Q_{1-\alpha}) = 1 - \alpha$. From Proposition 2 and the Continuous Mapping theorem, $\widehat{Q}_{1-\alpha}$ can replace $Q_{1-\alpha}$ for a Gaussian process. Thus, we can derive asymptotic SCBs for CDF $F_k(\cdot)$ for any fixed $k \in \mathbb{Z}_+$.

Corollary 1. *Under Assumptions (A1) and (A3) - (A7), for any $\alpha \in (0, 1)$ and fixed $k \in \mathbb{Z}_+$, as $n \rightarrow \infty$, an asymptotic $100(1 - \alpha)\%$ smooth simultaneous confidence band based on \widehat{F}_{nk} for F_k and nonsmooth simultaneous confidence band based on \widehat{F}_{nk}^\dagger are respectively given by $\left[\widehat{F}_{nk} \pm n^{-1/2} \widehat{Q}_{1-\alpha} \right] \cap [0, 1]$ and $\left[\widehat{F}_{nk}^\dagger \pm n^{-1/2} \widehat{Q}_{1-\alpha} \right] \cap [0, 1]$.*

4.3 Uniform testing for FPC scores

The distribution of the test statistics S_n and S_n^\dagger can be well approximated by the distribution of $\max_{1 \leq k \leq \kappa_n} \sup_{x \in \mathbb{R}} |\mathcal{G}_k(x)|$ under the null hypothesis in (1.2), as shown in Theorem 4 and Theorem 5. Following the procedures outlined in subsection 4.2, we construct a sequence of random vectors $\left\{ \widehat{\Xi}_{ik}(z_l) \right\}_{l=1}^{L_k}$, $1 \leq i \leq n$, $1 \leq k \leq \kappa_n$ based on (4.12), in order to obtain $\widehat{\Sigma}_k(\cdot, \cdot)$. The L_k equally spaced grid points are determined by $\min \left\{ \min_{i=1}^n \widehat{\xi}_{ik}, -n^{1/8} \right\} = z_{k1} < z_{k2} < \cdots < z_{k, L_k} = \max \left\{ \max_{i=1}^n \widehat{\xi}_{ik}, n^{1/8} \right\}$, where $L_k = L_k(n)$ diverges to infinity with a polynomial

4.3 Uniform testing for FPC scores

rate as $n \rightarrow \infty$. For instance, we suggest $L_k(n) \asymp n$. After that, we generate $\sum_{k=1}^{\kappa_n} L_k$ -dimensional Gaussian random vectors with mean zero and covariance matrix: $\text{diag} \left(\left\{ \widehat{\Sigma}_1(z_{1l}, z_{1l'}) \right\}_{l,l'}^{L_1}, \left\{ \widehat{\Sigma}_2(z_{2l}, z_{2l'}) \right\}_{l,l'}^{L_2}, \dots, \left\{ \widehat{\Sigma}_{\kappa_n}(z_{\kappa_n,l}, z_{\kappa_n,l'}) \right\}_{l,l'}^{L_{\kappa_n}} \right)$. We repeat this process B times, where B is a large predetermined integer. Then, we compute the empirical upper α quantile of the maximal absolute value for each replication, denoted by $\widehat{Z}_{1-\alpha}$.

Besides, the test statistics V_n and V_n^\dagger converge weakly to the weighted sum of the squared L^2 -norms of Gaussian processes $\{\zeta_k(x)\}_{k=1}^{\kappa_n}$, as proved in Theorems 4 and 5. The squared L^2 -norm of $\zeta_k(x)$ is distributed as a weighted sum of chi-squared random variables $\sum_{m=1}^{\infty} b_{km} \chi_{km}^2$, where b_{km} are the eigenvalues of the covariance function Σ_k and $\{\chi_{km}^2\}_{m=1}^{\infty}$ are independent standard chi-squared random variables of degree 1. To approximate the distribution of the weighted sum of chi-squared, we compute the eigenvalues $\{\widehat{b}_{km}\}_{m=1}^{L_k}$ of the covariance matrix $\left\{ \widehat{\Sigma}_k(z_{kl}, z_{kl'}) \right\}_{l,l'}^{L_k}$ for all $1 \leq k \leq \kappa_n$ and use a truncated number $M_k \asymp \log n$ to simulate independent chi-squared random variables $\{\chi_{km}^2\}_{k=1, m=1}^{\kappa_n, M_k}$ repeatedly. The empirical upper α quantile of the weighted sum of chi-squared, denoted by $\widehat{U}_{1-\alpha}$, is obtained from the simulated data. The next proposition demonstrates our testing procedures are asymptotically correct.

Proposition 3. *Under Assumptions (A1)-(A7), for any given significance level $\alpha \in$*

$(0, 1)$, as $n \rightarrow \infty$, under H_0 in (1.2),

$$\mathbb{P}\left(S_n \leq \widehat{Z}_{1-\alpha}|\{Y_{ij}\}_{i=1,j=1}^{n,N}\right) \xrightarrow{\mathbb{P}} 1 - \alpha, \quad \mathbb{P}\left(S_n^\dagger \leq \widehat{Z}_{1-\alpha}|\{Y_{ij}\}_{i=1,j=1}^{n,N}\right) \xrightarrow{\mathbb{P}} 1 - \alpha, \quad (4.14)$$

$$\mathbb{P}\left(V_n \leq \widehat{U}_{1-\alpha}|\{Y_{ij}\}_{i=1,j=1}^{n,N}\right) \xrightarrow{\mathbb{P}} 1 - \alpha, \quad \mathbb{P}\left(V_n^\dagger \leq \widehat{U}_{1-\alpha}|\{Y_{ij}\}_{i=1,j=1}^{n,N}\right) \xrightarrow{\mathbb{P}} 1 - \alpha. \quad (4.15)$$

Under H_1 in (1.2),

$$\mathbb{P}\left(S_n > \widehat{Z}_{1-\alpha}|\{Y_{ij}\}_{i=1,j=1}^{n,N}\right) \xrightarrow{\mathbb{P}} 1, \quad \mathbb{P}\left(S_n^\dagger > \widehat{Z}_{1-\alpha}|\{Y_{ij}\}_{i=1,j=1}^{n,N}\right) \xrightarrow{\mathbb{P}} 1, \quad (4.16)$$

$$\mathbb{P}\left(V_n > \widehat{U}_{1-\alpha}|\{Y_{ij}\}_{i=1,j=1}^{n,N}\right) \xrightarrow{\mathbb{P}} 1, \quad \mathbb{P}\left(V_n^\dagger > \widehat{U}_{1-\alpha}|\{Y_{ij}\}_{i=1,j=1}^{n,N}\right) \xrightarrow{\mathbb{P}} 1. \quad (4.17)$$

5. Simulation

In this section, numerical simulation studies are conducted to investigate the finite-sample performance of the proposed methods. The data are generated from the following model: $Y_{ij} = m(j/N) + \sum_{k=1}^{\infty} \xi_{ik} \phi_k(j/N) + \sigma(j/N) \varepsilon_{ij}$, where $m(x) = 5 + \sin\{2\pi(x - 1/2)\}$ and $\{\xi_{ik}\}_{i=1,k=1}^{n,20}$ are i.i.d random variables. The rescaled eigenfunctions are defined as $\phi_k(x) = \sqrt{\lambda_k} \psi_k(x)$, where $\lambda_k = 5k^{-2}$ for $k = 1, 2, \dots, 20$ and $\lambda_k = 0$ for $k > 20$, and $\psi_{2k-1} = \sqrt{2} \sin(2k\pi x)$, $\psi_{2k} = \sqrt{2} \cos(2k\pi x)$ for $k \in \mathbb{Z}_+$. We consider two options for the standard deviation function: a homoscedastic case with $\sigma(x) = \sigma_\varepsilon$ and a heteroscedastic case with $\sigma(x) = 6/5\sigma_\varepsilon (5 + \exp(x))^{-1} (5 - \exp(x))$. The noise level is set at $\sigma_\varepsilon = 1$. We consider three error distributions: the standard

Normal distribution $N(0, 1)$, the Uniform distribution $U(-\sqrt{3}, \sqrt{3})$, and the standardized Laplace distribution with density $f(x) = 2^{-1/2} \exp(\sqrt{2}|x|)$. The number of grid observations N is set at 100, 200, 400, and 600, and the number of trajectories is $n = cN^\theta$ with $c = 0.8$ and $\theta = 1$.

To assess our SCBs for FPC score CDFs, we independently generate ξ_{ik} from either a standard Gaussian $N(0, 1)$ or a rescaled $t(10)$ distribution. We explore two cases for our hypothesis testing procedure (1.2): In Case 1, testing for normality with $F_k(\cdot) = \Phi(\cdot)$, ξ_{ik} is drawn from $N(0, 1)$, $U(-\sqrt{3}, \sqrt{3})$, or standardized Laplace distribution. In Case 2, testing if FPC score distribution is rescaled $t(10)$, ξ_{ik} comes from rescaled $t(10)$, $U(-\sqrt{3}, \sqrt{3})$, or standardized Laplace. For both cases, $\kappa_n = \lceil \log n \rceil$. Each experiment involves 1000 bootstrap replications for quantile estimation and 500 Monte Carlo replications.

Tables S.1-S.4 indicate that smooth SCBs based on \widehat{F}_{nk} slightly outperform non-smooth ones in coverage frequency, without width differences (Wang et al. (2013), Wang et al. (2014)). As sample size grows, empirical coverage rates align more with the nominal confidence level, supporting our asymptotic theory. Figures S.1 - S.2 display \widehat{F}_{nk} and \widehat{F}_{nk}^\dagger estimators and their SCBs for ξ_{1k} , showing narrower SCBs and estimators closer to the true CDF as N increases. Tables S.5-S.8 show the test's empirical size approaching 0.05 and power nearing 1 with increasing N . The nonsmooth estimator \widehat{F}_{nk}^\dagger shows slightly higher empirical power than \widehat{F}_{nk} , with little difference

across ε_{ij} distributions.

6. Application

6.1 Well-known functional data sets

The first dataset records the heights of 54 girls and 39 boys at 31 different ages, as shown in Figure S.3, and it is a part of object *growth* in the *fda* package; see Ramsay et al. (2022). Since height is continuously changing with time, it can be modeled as functional data with measurement errors. In the field of biology, there is interest in the patterns of variation in the growth curves of males and females. Thus, we apply the proposed methods to investigate this issue.

To analyze the growth curves of boys, the default value of $\kappa_n = \lceil \log n \rceil$ is used, resulting in $\kappa_n = 4$. The first four estimated eigenvalues are 30.937, 1.555, 1.065, and 0.679, respectively, which account for more than 99% of the variation in the data. For the curves of girls, the default value of $\kappa_n = 4$ is also used, and the first four estimated eigenvalues are 29.090, 2.299, 0.726, and 0.378, explaining more than 99% of the variation in the data. Therefore, we construct the SCBs for the CDF of the first four FPC scores for both sets of curves, which are presented in Figures S.4- S.5.

We then address Assumption (A6), which imposes the independence of FPC scores ξ_{ik} 's across k . A natural approach involves estimating these scores and subsequently employing an independent test. In this regard, we apply a K-sample test-

ing method as proposed in Bakirov et al. (2006) and facilitated by the R package `IndependenceTests`. The resulting statistic is 0.534, respectively. Notably, the corresponding critical value for a significance level of 0.05 is 0.822. Consequently, we can confidently conclude that the FPC scores of the growth curves exhibit independence over k . Subsequently, we test whether the distributions of FPC scores for growth curves in boys and girls are equal using a two-sample testing procedure. We also check whether the data can be assumed to follow a Gaussian process in the space $L^2[0, 1]$ using our testing procedures and the JB test proposed in Górecki et al. (2020). Results in Table 1 suggest no strong evidence of differences in the distribution of FPC scores between boys and girls, or that the growth curves are not Gaussian. Therefore, we conclude that the growth curves of boys and girls belong to the family of Gaussian distributions. Once the curve data are verified as Gaussian processes, one only need to model the mean function and covariance function to fully characterize the properties of distributions.

The second dataset, containing spectral curves for 215 meat samples, is available in the *fda.usc* package as *tecator*. The data are recorded on a Tecator Infracotec Food and Feed Analyzer working in the wavelength range 850-1050 nm by the near infrared transmission principle. The varying fat content in each meat sample results in a different near infrared absorbance spectrum. To explain at least 99.5% of the variance of curves, we estimate the eigensystem with $\kappa_n = 2$ eigenvalues. We investigate the

6.1 Well-known functional data sets

Table 1: Two-sample tests and normality tests for two curves sets with the corresponding p -values in the brackets. $S_n, S_n^\circ (S_n^\dagger, S_n^\ddagger) [V_n, V_n^\circ (V_n^\dagger, V_n^\ddagger)]$: the KS-type [CVM-type] test statistics based on the smooth (non-smooth) estimator; JB : the JB -test statistic proposed in Górecki et al. (2020).

	S_n°	S_n^\dagger	V_n°	V_n^\ddagger	-
Two-sample	0.843(0.718)	0.818(0.768)	59.445(0.072)	59.220(0.072)	-
	S_n	S_n^\dagger	V_n	V_n^\dagger	JB
Boys	0.652(0.589)	0.671(0.530)	9.883(0.159)	9.472(0.180)	4.056(0.398)
Girls	0.837(0.216)	0.944(0.091)	11.450(0.183)	11.194(0.192)	3.750(0.441)

normality of the data using the CDF of the first FPC score and its SCBs in Figure S.6. The CDF of standard normal random variables falls outside the SCB, suggesting that normality of the data is questionable. Table 2 confirms this by showing that the null hypothesis of normality (1.3) is strongly rejected. We observe that some outlier curves have higher spectral absorbance than others, which may contribute to the lack of normality in the data. Then, we approximate the CDF of the first FPC score ξ_{i1} as a centralized gamma distribution with a shape parameter of 2.831 and a scale parameter of 0.594, and the CDF of the second FPC score $\xi_{i2}, i = 1, 2, \dots, n$, as a standard normal distribution. To test this approximation, we consider the hypothesis testing problem:

$$H_0 : F_1(x) = G(x), F_2(x) = \Phi(x), \text{ v.s. } H_1 : F_1(x) \neq G(x) \text{ or } F_2(x) \neq \Phi(x), \quad (6.18)$$

where $G(\cdot)$ is the CDF of the centralized gamma distribution mentioned above.

Table 2: Tests for the spectral curves with the corresponding p -values in the brackets. S_n , (S_n°) [V_n , (V_n°)]: the KS-type [CVM-type] test statistics based on the smooth (non-smooth) estimator; JB : the JB -test statistic proposed in Górecki et al. (2020).

the null	S_n	S_n^\dagger	V_n	V_n^\dagger	JB
(1.3)	1.240(0.021)	1.233(0.022)	0.388(0.000)	0.387(0.000)	210.295(0.000)
(6.18)	0.877(0.218)	0.867(0.227)	0.035(0.742)	0.038(0.696)	-

Through conducting the introduced independence test, we assert that the FPC scores are independent over k at the 95% confidence level, with the test statistic being 0.739 and the critical value being 0.762. Table 2 reports the test statistics and corresponding p -values obtained by applying our proposed testing procedure. The result supports the conclusion that the *tecator* data does not follow a Gaussian distribution, as the first FPC score may be drawn from a centralized gamma distribution. Given that the proposed test implies the skewness of the spectral curves of meat, using some robust functional data analysis methods combined with M-estimation might be a more reasonable choice for further data analysis. For instance, one could apply the clustering procedure for a non-Gaussian process developed in Zhong et al. (2021), or adopt the robust functional principal component analysis in Shi and Cao (2022).

6.2 EEG data

To further illustrate the proposed inference methods, we consider to study Electroencephalogram (EEG) data, which is known for containing substantial information about the function of the human brain. The data were collected by the research

group of Prof. Linhong Ji at the Department of Mechanical Engineering of Tsinghua University, and have been previously analyzed in several studies; see Li and Yang (2022), Zhong and Yang (2022), and Song et al. (2022). This dataset consists of EEG signals recorded from 32 scalp locations at a 1000Hz sample rate for 142 individuals during a five-minute closed-eye resting state experiment. We use the mid-200 signals of each individual from the 10-th scalp location and model the data using (1.1) with $n = 142$ and $N = 200$. Applying the estimation procedure, we recover the trajectories using a B-spline smoother. Figure S.8 shows segments of raw EEG data for 6 randomly selected participants, along with the corresponding B-spline estimation.

To investigate the normality assumption of the EEG data in the L^2 space, we apply the normality test in (1.3) with $\kappa_n = 7$, as suggested by Song et al. (2022). According to the discussion of independence testing of FPC scores in Section 6.1, we obtain the test statistic of 0.817 and the rejection region of 0.899, which provide evidence that the FPC scores are independent over k . The results of the proposed CVM-type testing procedures and the JB test in Górecki et al. (2020) are displayed in Table 3. Both tests strongly reject the null hypothesis (1.3), indicating that the EEG data does not follow a Gaussian process in the L^2 space. We also present the proposed SCBs for the CDF of the first six FPC scores in Figure S.9, which suggests that the first three FPC scores follow the standardized Laplace distribution with CDF $\mathcal{L}(\cdot)$, while the last four FPC scores can be considered Gaussian. Therefore,

Table 3: Tests for the EEG data with the corresponding p -values in the brackets. S_n , (S_n°) [V_n , (V_n°)]: the KS-type [CVM-type] test statistics based on the smooth (non-smooth) estimator; JB : the JB -test statistic proposed in Górecki et al. (2020).

the null	S_n	S_n^\dagger	V_n	V_n^\dagger	JB
(1.3)	0.969(0.201)	0.943(0.245)	27.945(0.001)	28.231(0.001)	119.674(0.000)
(6.19)	0.721(0.802)	0.745(0.738)	9.123(0.604)	9.420(0.557)	-

we test the null hypothesis:

$$\begin{aligned}
 H_0 : F_k(x) = \mathcal{L}(x) \quad 1 \leq k \leq 3 \text{ and } F_k(x) = \Phi(x) \quad 4 \leq k \leq 7, \\
 H_1 : F_{k_1}(x) \neq \mathcal{L}(x) \quad \exists 1 \leq k_1 \leq 3 \text{ or } F_{k_2}(x) \neq \Phi(x) \quad \exists 4 \leq k_2 \leq 7.
 \end{aligned} \tag{6.19}$$

Table 3 confirms this finding, which guides us in gaining a deeper understanding of the distribution of the EEG data.

7. Concluding Remark

In this paper, we present a novel method for estimating the CDF of FPC scores in densely observed functional data. We introduce both smooth and non-smooth estimators for the CDF, which are asymptotically equivalent and possess advantageous properties under mild conditions. Utilizing Theorems 3 and 5, we construct SCBs for the CDF of FPC scores. Our method also includes a new testing procedure for the distribution of FPC scores, accommodating the sample size's growth and the functional data's infinite-dimensional character. This includes testing for the nor-

quality of functional data. We assess our approach through simulation studies and its application to well-known functional datasets and EEG data. Future research could expand this method to other functional data types like image data, sphere or manifold data, functional time series, or spatially indexed functional data.

Acknowledgements

This research has been partially supported by National Natural Science Foundation of China award 12171269.

Supplementary Material

Supplementary Material contains additional tables and figures in Sections 5-6 and detailed proofs of the theoretical results with necessarily technical lemmas.

References

- Bakirov, N. K., M. L. Rizzo, and G. J. Székely (2006). A multivariate nonparametric test of independence. *Journal of multivariate analysis* 97(8), 1742–1756.
- Berkes, I., R. Gabrys, L. Horváth, and P. Kokoszka (2009). Detecting changes in the mean of functional observations. *J. R. Stat. Soc. B* 71(5), 927–946.
- Bickel, P. J. and M. Rosenblatt (1973). On some global measures of the deviations of density function estimates. *Ann. Stat.* 1(6), 1071–1095.

- Bosq, D. (2000). *Linear processes in function spaces: theory and applications*, Volume 149. Springer Science & Business Media, New York.
- Cai, L. and Q. Hu (2024). Simultaneous inference and uniform test for eigensystems of functional data. *Computational Statistics & Data Analysis*, 107900.
- Cai, T. T. and P. Hall (2006). Prediction in functional linear regression. *Ann. Stat.* 34(5), 2159–2179.
- Cao, G., L. Yang, and D. Todem (2012). Simultaneous inference for the mean function based on dense functional data. *J. Nonparametr. Stat.* 24(2), 359–377.
- Chen, M. and Q. Song (2015). Simultaneous inference of the mean of functional time series. *Electron. J. Stat.* 9(2), 1779–1798.
- Constantinou, P., P. Kokoszka, and M. Reimherr (2017). Testing separability of space-time functional processes. *Biometrika* 104(2), 425–437.
- Dauxois, J., A. Pousse, and Y. Romain (1982). Asymptotic theory for the principal component analysis of a vector random function: some applications to statistical inference. *J. Multivariate Anal.* 12(1), 136–154.
- De Boor, C. (1978). *A practical guide to splines*, Volume 27. springer-verlag, New York.

REFERENCES

- Fremdt, S., L. Horváth, P. Kokoszka, and J. G. Steinebach (2014). Functional data analysis with increasing number of projections. *Journal of Multivariate Analysis* 124, 313–332.
- Ghale-Joogh, H. S. and S. M. E. Hosseini-Nasab (2018). A two-sample test for mean functions with increasing number of projections. *Statistics* 52(4), 852–873.
- Górecki, T., S. Hörmann, L. Horváth, and P. Kokoszka (2018). Testing normality of functional time series. *J. Time Ser. Anal.* 39(4), 471–487.
- Górecki, T., L. Horváth, and P. Kokoszka (2020). Tests of normality of functional data. *Int. Stat. Rev.* 88(3), 677–697.
- Hall, P. and M. Hosseini-Nasab (2009). Theory for high-order bounds in functional principal components analysis. *Math. Proc. Cambridge* 146(1), 225–256.
- Hörmann, S., P. Kokoszka, and T. Kuenzer (2022). Testing normality of spatially indexed functional data. *Can. J. Stat.* 50(1), 304–326.
- Hörmann, S., P. Kokoszka, and G. Nisol (2018). Testing for periodicity in functional time series. *Ann. Stat.* 46(6A), 2960–2984.
- Hsing, T. and R. Eubank (2015). *Theoretical foundations of functional data analysis, with an introduction to linear operators*, Volume 997. John Wiley & Sons, New York.

REFERENCES

- Hu, Q. and J. Li (2024). Statistical inference for mean function of longitudinal imaging data over complicated domains. *Statistica Sinica*.
- Kokoszka, P. and M. Reimherr (2013). Asymptotic normality of the principal components of functional time series. *Stoch. Proc. Appl.* 123(5), 1546–1562.
- Li, J. and L. Yang (2022). Statistical inference for functional time series. *Stat. Sinica*.
DOI: 10.5705/ss.202021.0107.
- Li, Y. and T. Hsing (2010). Uniform convergence rates for nonparametric regression and principal component analysis in functional/longitudinal data. *The Annals of Statistics* 38(6), 3321 – 3351.
- Liang, D., H. Huang, Y. Guan, and F. Yao (2022). Test of weak separability for spatially stationary functional field. *Journal of the American Statistical Association*, 1–14.
- Neumeier, N. and I. Van Keilegom (2010). Estimating the error distribution in nonparametric multiple regression with applications to model testing. *Journal of Multivariate Analysis* 101(5), 1067–1078.
- Ramsay, J. O., S. Graves, and G. Hooker (2022). *fda: Functional Data Analysis*. R package version 6.0.5.

REFERENCES

- Shi, H. and J. Cao (2022). Robust functional principal component analysis based on a new regression framework. *Journal of Agricultural, Biological and Environmental Statistics* 27(3), 523–543.
- Song, Z., L. Yang, and Y. Zhang (2022). Hypotheses testing of functional principal components. *Manuscript*.
- Wang, J., F. Cheng, and L. Yang (2013). Smooth simultaneous confidence bands for cumulative distribution functions. *J. Nonparametr. Stat.* 25(2), 395–407.
- Wang, J., R. Liu, F. Cheng, and L. Yang (2014). Oracally efficient estimation of autoregressive error distribution with simultaneous confidence band. *Ann. Stat.* 42(2), 654–668.
- Wang, J. and L. Yang (2009). Polynomial spline confidence bands for regression curves. *Stat. Sinica* 19(1), 325–342.
- Wang, Q., S. Guo, F. Yao, and C. Zou (2022). Thresholding mean test for functional data with power enhancement. *Stat* 11(1), e509.
- Yao, F., H.-G. Müller, and J.-L. Wang (2005a). Functional data analysis for sparse longitudinal data. *J. Am. Stat. Assoc.* 100(470), 577–590.
- Yao, F., H.-G. Müller, and J.-L. Wang (2005b). Functional linear regression analysis for longitudinal data. *Ann. Stat.* 33(6), 2873–2903.

REFERENCES

Zhang, H. and Y. Li (2021). Unified principal component analysis for sparse and dense functional data under spatial dependency. *J. Bus. Econ. Stat.*.

Zhang, X., X. Shao, K. Hayhoe, and D. J. Wuebbles (2011). Testing the structural stability of temporally dependent functional observations and application to climate projections. *Electron. J. Stat.* 5, 1765–1796.

Zhong, C. and L. Yang (2022). Statistical inference for functional time series: Autocovariance function. *Stat. Sinica*. DOI: 10.5705/ss.202021.0121.

Zhong, Q., H. Lin, and Y. Li (2021). Cluster non-gaussian functional data. *Biometrics* 77(3), 852–865.

Center for Statistical Science and Department of Industrial Engineering, Tsinghua University, Beijing 100084, China.

E-mail: cailh22@mails.tsinghua.edu.cn

Center for Statistical Science and Department of Industrial Engineering, Tsinghua University, Beijing 100084, China.

E-mail: hqr20@mails.tsinghua.edu.cn